ISSN 0006-2979, Biochemistry (Moscow), 2026, Vol. 91, No. 10, pp. 1937-1950 © Pleiades Publishing, Ltd., 2026.

Strategies for Overcoming Acquired Resistance of Tumor Cells to MDM2 Inhibitors

Nikolay V. Pervushin[1,2], Ekaterina S. Prosandeeva[1,2], Boris Zhivotovsky[1,2,3,a]*, and Gelina S. Kopeina[1,b]*

[1]*Engelhardt Institute of Molecular Biology, Russian Academy of Sciences, 119991 Moscow, Russia*
[2]*Faculty of Fundamental Medicine, Lomonosov Moscow State University, 119991 Moscow, Russia*
[3]*Institute of Environmental Medicine, Karolinska Institutet, 17177 Stockholm, Sweden*
[a]*e-mail: boris.zhivotovsky@ki.se* [b]*e-mail: lirroster@gmail.com*

Received June 5, 2026
Revised June 29, 2026
Accepted July 14, 2026

Abstract—Emergence of drug resistance remains a major challenge in oncology and is closely associated with tumor progression. Activation of the tumor-suppressive activity of p53 through selective inhibition of its negative regulator MDM2 is a promising strategy for anticancer therapy. MDM2 antagonists, which have been extensively evaluated in clinical trials over the past two decades, could lose efficacy because tumor cells acquire resistance to these agents. We found that SH-SY5Y neuroblastoma cells resistant to the MDM2 antagonist RG7388 were less sensitive to ferroptosis induction and showed alterations in cell cycle distribution. In addition, both parental and resistant cells were highly sensitive to autophagy induction. Finally, combining RG7388 with various inhibitors of cellular metabolism and other anticancer compounds increased its cytotoxicity and could facilitate partial or complete overcoming of this type of resistance.

DOI: 10.1134/S0006297926601875

Keywords: drug resistance, MDM2, p53, RG7388, tumor cells, chemotherapy

INTRODUCTION

Evasion of different types of programmed cell death (PCD), including apoptosis, is an important feature of tumor cells, which promotes cancer progression [1, 2]. Effective induction of apoptosis therefore underlies many anticancer strategies. One such strategy targets the transcription factor p53, which is a key regulator of cellular functions [3-5]. p53 controls multiple intracellular signaling pathways by altering the expression of a broad range of genes involved in DNA repair, the cell cycle, metabolism, and cellular senescence. It also regulates apoptosis through several mechanisms, including increased expression of proapoptotic proteins of the B-cell lymphoma 2 (Bcl-2) family [6, 7].

Under unstressed conditions, various cell types maintain low levels of the p53 protein through the action of the E3 ubiquitin ligase mouse double minute 2 homolog (MDM2) [5]. Negative MDM2-mediated regulation of p53 occurs through several mechanisms, the principal one being MDM2-dependent proteasomal degradation of p53 [8]. MDM2 also disrupts the p53-DNA interactions, promotes its nuclear export, and negatively regulates p53 transcription [9, 10]. In addition, an increase in the intracellular p53 levels induces expression of the MDM2 gene, providing an additional mechanism for self-regulation of p53 levels in cells [5, 8]. Mouse double minute 4/X homolog (MDMX/MDM4), a protein related to MDM2, also contributes to the negative regulation of p53 [11, 12].

p53 could fail to suppress tumor growth for two main reasons. First, the *TP53* gene is highly susceptible to mutation, and approximately half of human tumors harbor functionally significant mutations in *TP53* [5]. Molecules that reactivate mutant p53 have been developed for such tumors [4, 13]. Second, p53 activity could be suppressed by an increased activity of its negative regulators, MDM2 and MDMX/MDM4, whose genes could be amplified in some tumors [14, 15].

* To whom correspondence should be addressed.

Antagonists of MDM2 and/or MDMX/MDM4 have therefore been proposed for the tumors expressing the wild-type p53 [3]. Both reactivators and MDM2 antagonists have been studied extensively over the past several decades, including in clinical trials [3-5, 8].

Unfortunately, as noted above, many drugs, particularly anticancer agents, lose their efficacy because tumor cells acquire resistance. This phenomenon has also been demonstrated for the drugs of the MDM2 antagonist set [16-19]. Earlier, we generated SH-SY5Y neuroblastoma cells with acquired resistance to the MDM2 antagonist RG7388, which has been repeatedly evaluated in clinical trials [19]. We found that this type of resistance was associated with the emergence of a mutation in the *TP53* gene that led to the His193Arg amino acid substitution. The mutation destabilized p53 and impaired its interaction with DNA, thereby reducing p53 transcriptional activity and decreasing accumulation of the p53, MDM2, and p53-inducible proteins, including p21 and Puma. In addition, we showed that the resistant cells were less sensitive to cisplatin and doxorubicin *in vitro* and *in vivo* and became more "aggressive", that is, demonstrated a higher proliferation rate and more active metabolism in comparison with the parental cells [19], which is consistent with the existing evidence that acquisition of the p53 mutations could be accompanied by the additional modifications that enhance malignancy of the mutant clones – the so-called "gain-of-function" effect [20-22].

The present study revealed additional aspects of acquired resistance to RG7388 in cells carrying the p53 His193Arg substitution. The aims were to assess the contribution of other forms of PCD to this type of drug resistance, evaluate the potential of targeting metabolism of the resistant clones, and determine whether other anticancer agents could facilitate overcoming of the resistance. Because we previously found that this mutation occurs spontaneously in various types of human tumors, further studies of the cells carrying this mutation could clarify its potential consequences for the patients.

MATERIALS AND METHODS

Cell culture. SH-SY5Y neuroblastoma cells were obtained from the Division of Toxicology, Karolinska Institutet (Stockholm, Sweden). Cells were cultured in DMEM containing 4.5 g/L glucose, sodium pyruvate, and glutamine (PanEco, Russia). The medium was supplemented with 10% fetal bovine serum (Gibco, USA), 100 U/mL penicillin, and 100 U/mL streptomycin. Cells were maintained at 37°C in a humidified atmosphere containing 5% CO_2. Experiments were performed when the cell cultures reached at least 70% confluence. Growing cells were regularly tested for mycoplasma contamination using a MycoReport kit (Evrogen, Russia). Cell numbers were evaluated using a Countess Automated Cell Counter (Thermo Scientific, USA).

Reagents. Cells were cultured for 24 h after seeding. The culture medium was then replaced, and the following compounds were added: an MDM2 antagonist RG7388 (Roche, Switzerland), a DNA-damaging agent etoposide (Teva Pharmaceutical, Israel), an antimitotic agent colchicine, a multikinase inhibitor sunitinib malate, an electron transport chain (ETC) complex I inhibitor rotenone, an ATP synthase inhibitor oligomycin, a glycolysis inhibitor 2-deoxyglucose, and autophagy inhibitors bafilomycin A1 and chloroquine. Unless otherwise indicated, all compounds were obtained from Sigma, USA. Autophagy was induced using a glucose-containing Hanks' balanced salt solution (HBSS) lacking amino acids and serum (Gibco). Ferroptosis was induced with imidazole ketone erastin (IKE) (MedChemExpress, USA) and inhibited with ferrostatin-1 (Sigma). Necroptosis was induced using a TBZ combination, which contained tumor necrosis factor alpha (TNF-α) (MedChemExpress), BV6 (MedChemExpress), and z-VAD-FMK (zVAD; Bachem, Switzerland). Necroptosis was inhibited with necrostatin-1s (Selleckchem, USA). Control cells received the corresponding vehicle. Detailed experimental conditions are provided in the Results section and in Table S1 from the Online Resource 1.

MTT assay. Cells were seeded in 96-well plates (Nunc, Denmark) at a density of 10,000 cells per well and treated as described above. After 24 h, 100 μL of a fresh serum-free DMEM containing MTT reagent at a final concentration of 0.45 mg/mL was added to each well. Cells were incubated for 2.5-3 h at 37°C. The medium was then removed, and 100 μL of dimethyl sulfoxide (PanEco) was added to dissolve the formazan crystals. Absorbance was measured at 570 nm using a Varioskan Flash microplate reader (Thermo Scientific), with 650 nm as the reference wavelength. Cell viability was calculated from the background-corrected absorbance value (A_{570}-A_{650}) and normalized to the corresponding control.

Live/dead assay. Cell viability was assessed using the Live/Dead assay based on dual fluorescent staining with calcein AM and ethidium homodimer-1 (EthD-1; both from LumiProbe, Russia). Cells were seeded in 24-well glass-bottom plates (Greiner Bio-One, Austria) at a density of 130,000 cells per well. Cells were treated as described in the "Reagents" subsection. After treatment, cells were stained directly in DMEM without replacing the medium. For this, calcein AM and ethidium homodimer-1 were added to the medium to final concentrations of 2 μM and 4 μM,

respectively. Cells were then incubated for 15 min at 37°C in the dark.

Images were acquired using a confocal imaging system based on an inverted Nikon ECLIPSE Ti2 microscope (Nikon Instruments Inc., USA) equipped with a ×20 objective. Calcein AM fluorescence was detected using 488-nm excitation and a 500-550-nm emission range. EthD-1 fluorescence was detected using 561-nm excitation and a 600-650-nm emission range. At least 18 fields of view from different areas of each well were imaged.

Images were analyzed using CellProfiler. Live and dead cells were segmented separately based on calcein AM and EthD-1 fluorescence, respectively. The numbers of live (live_count) and dead (dead_count) cells were determined for each field. Percentages of live and dead cells were calculated as follows: % live cells = live_count/(live_count + dead_count) × 100%; % dead cells = dead_count/(live_count + dead_count) × 100%. Values for each well were calculated using data from all acquired fields.

Western blot analysis. Cells were seeded into 35 mm Petri dishes (SPL Lifesciences, South Korea) at a density of 500,000 cells per dish. After 24–36 hours of seeding, the culture medium was replaced with fresh medium, and the appropriate reagents specified in the text and in Table S1 from the Online Resource 1 were added. Cells were detached from Petri dishes using a scraper, collected by centrifugation, washed with cold phosphate-buffered saline, and centrifuged again. Cell pellets were resuspended in a RIPA lysis buffer and incubated on ice for 20 min. The lysates were clarified by centrifugation, and samples for Western blot analysis were prepared as described previously [23].

The following primary antibodies were used: against poly(ADP-ribose) polymerase (PARP) (ab74290), p62 (ab56416), LC3B (ab51520), and Vinculin (ab129002) from Abcam, United Kingdom; against p53 (P6874-200UL) from Sigma-Aldrich; and against cleaved PARP (p89; #5625), caspase-3 (#9662), glyceraldehyde-3-phosphate dehydrogenase (GAPDH) (#2118), and p21 Waf1/Cip1 (#2946) from Cell Signaling, USA. An anti-mouse IgG (#515-035-062) and anti-rabbit IgG (#111-035-144) secondary antibodies were obtained from Jackson ImmunoResearch, USA.

Protein levels were quantified by densitometry and normalized to GAPDH as a loading control. Images were analyzed using ImageJ version 1.53t.

Flow-cytometric analysis of cell-cycle distribution. Cells were detached from Petri dishes (SPL Lifesciences) by trypsinization, collected by centrifugation, washed with cold phosphate-buffered saline, and fixed in ice-cold 70% ethanol prepared in phosphate-buffered saline. After removal of ethanol, cells were stained with 50 μg/mL propidium iodide and 100 μg/mL RNase A (both from Thermo Fisher Scientific, USA). Next, the measurements were performed using a BD FACSCanto II flow cytometer (BD Biosciences, USA), as described previously [24]. Cell-cycle distribution was analyzed using the Floreada.io software (https://floreada.io).

Real-time polymerase chain reaction (PCR). Total RNA was isolated using TRIzol reagent (Thermo Fisher Scientific). Reverse transcription was performed using an MMLV RT kit (Evrogen). The resulting cDNA was used for real-time PCR with primers specific for p21/CDKN1A or TATA-binding protein and a qPCRmix-HS SYBR reagent (Evrogen). The sequences of the primers used for amplification of CDKN1A and TBP are presented in Table S2 from the Online Resource 1. p21 mRNA expression was measured using a CFX96 Real-Time PCR Detection System (Bio-Rad, USA), as described previously [24].

Statistical analysis. Statistical significance was assessed using the Mann–Whitney U test. Data processing and statistical analyses were performed using Microsoft Excel and GraphPad Prism 6 (GraphPad Software, USA). Data in bar graphs are presented as mean ± standard deviation of four independent biological replicates. Differences were considered statistically significant at $p < 0.05$.

RESULTS

Characterization of neuroblastoma cells with acquired resistance to the MDM2 antagonist RG7388. We previously used SH-SY5Y neuroblastoma cells to generate a cell population that is resistant to the MDM2 antagonist RG7388 [19]. This model was selected for two reasons. First, SH-SY5Y cells express the wild-type p53, which is required for the MDM2 antagonist activity [4, 25]. Second, these cells are highly sensitive to MDM2 inhibition [26, 27]. The resistant SH-SY5Y-Res cells were generated using a pulse-selection method described previously [19, 24, 28, 29]. Briefly, this approach was used because of its clinical relevance, as it involves growing the parental cells with gradually increasing concentrations of the test compound (the “treatment period”), alternating with cultivation of the cells without the anticancer drug (the “recovery period”). Thus, the pulse method mimics treatment cycles administered to the cancer patients [30]. Differences in sensitivity to RG7388 between the parental and resistant neuroblastoma cells remained stable over time. Live/Dead analysis showed a smaller reduction in the number of live cells and a smaller increase in the number of dead cells in the SH-SY5Y-Res cells in comparison with the parental SH-SY5Y cells after MDM2 inhibition (Fig. 1, a-c). Western blot analysis confirmed these findings (Fig. 1d).

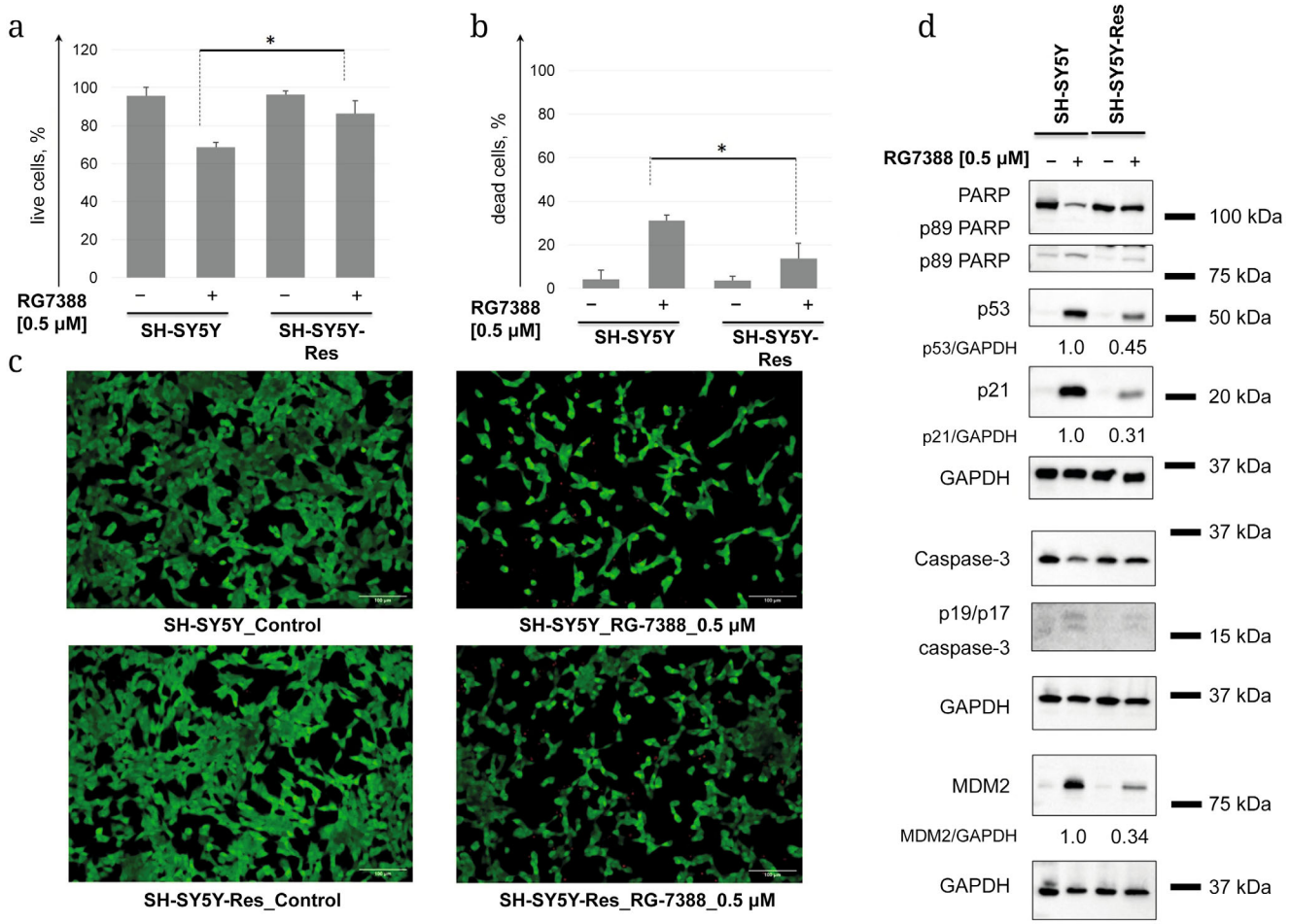

Fig. 1. Analysis of the efficacy of the MDM2 antagonist RG7388 (0.5 μM) in SH-SY5Y and SH-SY5Y-Res cells. Results of cell viability assessment by the Live/Dead assay (a, b) with representative images (c) and Western blot analysis (d) in SH-SY5Y and SH-SY5Y-Res cells. Incubation period: 24 h. Data (a, b) are presented as a mean ± standard deviation, $n = 4$; * $p < 0.05$ (U-test).

The parental cells showed more extensive processing of caspase-3 and cleavage of its substrate PARP, both markers of apoptosis [31, 32]. This was indicated by the decreased levels of the full-length proteins and accumulation of the catalytically active p19/17 caspase-3 (catalytically active fragments of the effector caspase-3) and p89 PARP fragments. Western blot analysis also revealed differences between the parental SH-SY5Y cells and SH-SY5Y-Res cells in the RG7388-induced accumulation of p53, its negative regulator MDM2, and the p53-inducible protein p21, a marker of p53 activation [33] (Fig. 1d).

As noted above, we previously showed that the acquired resistance of neuroblastoma cells to RG7388 was associated with a mutation in the *TP53* gene involving the His193Arg substitution in the p53 protein, which impaired p53 stability and function [19]. We also found no contribution of the multidrug resistance protein 1 (MDR1)-encoded P-glycoprotein, which mediates efflux of various compounds from the cells and frequently contributes to reduced drug efficacy [34]. In the present study, we analyzed the potential contribution of the Bcl-2 family proteins to this type of resistance, as increased levels of antiapoptotic proteins and/or decreased levels of proapoptotic proteins could reduce the sensitivity of malignant cells to anticancer agents [24, 35, 36]. Levels of the proapoptotic proteins Bak (Bcl-2 homologous antagonist/killer) and Bax (Bcl-2-associated X protein) and the antiapoptotic proteins Mcl-1 (myeloid cell leukemia 1), Bcl-xL (B-cell lymphoma-extra-large), and Bcl-2 did not differ prominently between the RG7388-resistant and parental cells. All observed differences were less than 10% (Fig. S1 in the Online Resource 1).

To confirm acquired resistance, we used several experimental approaches, including flow cytometric analysis of the sub-G1 population. Across a broad concentration range, the proportion of sub-G1 cells was significantly lower in SH-SY5Y-Res cells than in the parental ones [19]. Considering that the MDM2 antagonists affect cell cycle progression by stabilizing p53, we compared proportions of cells in the G1, S,

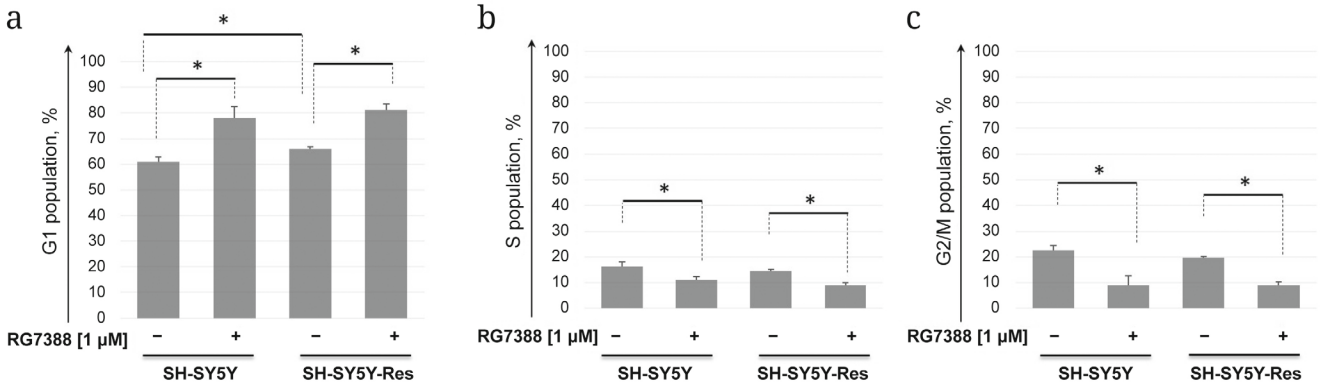

Fig. 2. Comparative analysis of cell cycle phase distribution upon addition of the MDM2 antagonist RG7388 (1 μM) to SH-SY5Y and SH-SY5Y-Res cells. Proportion of cells in the G1 (a), S (b), and G2/M (c) phases. Incubation period: 24 h. Data are presented as a mean ± standard deviation, $n = 4$; * $p < 0.05$ (U-test).

and G2/M phases. Addition of RG7388 increased the proportion of cells in the G1 phase and decreased the proportions of cells in the S and G2/M phases in both parental and resistant neuroblastoma cells (Fig. 2, a-c; Fig. S2 in the Online Resource 1). In untreated cells, the proportion of cells in G1 was higher in SH-SY5Y-Res cells than in parental SH-SY5Y cells (Fig. 2a). This finding indicates that acquisition of the resistant phenotype shifted the basal cell-cycle distribution toward G1, even in the absence of RG7388.

Assessment of the contribution of other types of PCD to the development of acquired resistance of tumor cells to the MDM2 antagonist RG7388. During the acquisition of resistance to anticancer agents, malignant cells could become less sensitive not only to apoptosis but also to other forms of PCD [37]. We therefore compared the parental SH-SY5Y cells and the resistant SH-SY5Y-Res cells after induction or inhibition of ferroptosis, necroptosis, and autophagy. In the Live/Dead assay, the ferroptosis inducer IKE (10 μM) significantly reduced the viability of parental SH-SY5Y cells. The ferroptosis inhibitor ferrostatin-1 (2 μM) prevented this effect. In contrast, ferrostatin-1 did not confer similar protection in SH-SY5Y-Res cells (Fig. 3). These results suggest that SH-SY5Y-Res cells are less sensitive to ferroptosis. At the same time, induction of necroptosis with a combination of TNF-α, BV6, and zVAD (TBZ; 10 ng/mL TNF-α, 500 nM BV6, and 20 μM zVAD) did not reduce the viability of either parental or resistant neuroblastoma cells (Fig. S3 in the Online Resource 1). These results indicate that SH-SY5Y-Res cells could be resistant to ferroptosis and that both cell lines are insensitive to necroptosis.

Next, the contribution of autophagy to the development of this type of resistance was assessed. Autophagy was induced by growing the cells under nutrient-deprivation conditions in HBSS, which contains neither amino acids nor fetal bovine serum [38]. The HBSS-induced autophagy was confirmed by the decreased levels of p62 and LC3 proteins, including LC3-I and LC3-II (Fig. 4a), which are classical markers of autophagic processes [39]. The MTT assay showed that growth in HBSS markedly reduced the viability of neuroblastoma cells. This effect was more pronounced in the resistant population, although results of Western blot analysis showed only minimal cleavage of apoptotic markers (Fig. 4a). Notably, the MTT assay and similar techniques measure overall cell viability, including proliferative and metabolic activity [28, 40]. These findings suggest that culturing in HBSS did not induce substantial apoptotic death in SH-SY5Y or SH-SY5Y-Res cells. Instead, it could have suppressed their proliferation and/or metabolism or stimulated nonapoptotic forms of PCD. In addition, culturing in HBSS enhanced the cytotoxic effect of RG7388 in both parental and resistant SH-SY5Y cells (Fig. 4b).

Autophagy was inhibited using bafilomycin A1 and chloroquine. Inhibition was confirmed by accumulation of the p62 and LC3-II proteins (Fig. S4, a and b in the Online Resource 1). Western blot and MTT analyses showed that both compounds induced processing of caspase-3 and cleavage of PARP and reduced viability of parental SH-SY5Y cells when used as single agents. In SH-SY5Y-Res cells, these effects were more pronounced with bafilomycin A1 than with chloroquine. Furthermore, exposure to bafilomycin A1 increased RG7388-induced cell death in both parental and resistant cells, whereas chloroquine produced this effect only in parental neuroblastoma cells (Fig. S4 in the Online Resource 1). Thus, the response of RG7388-resistant neuroblastoma cells to autophagy inhibition depended on the intrinsic cytotoxicity of the inhibitor.

Analysis of the efficacy of metabolic inhibitors for overcoming resistance of neuroblastoma cells to RG7388. As noted above, the SH-SY5Y-Res cells exhibit higher metabolic activity, including glycolysis

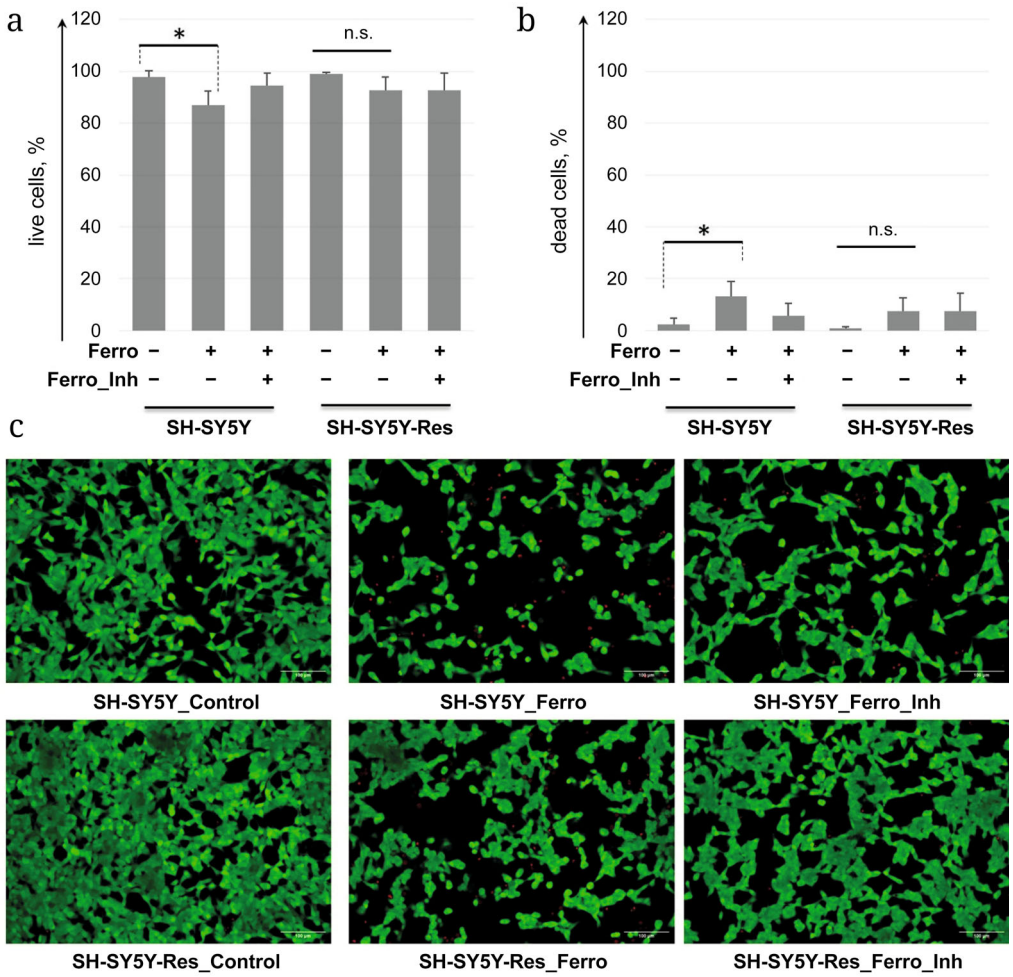

Fig. 3. Comparative analysis of the sensitivity of SH-SY5Y and SH-SY5Y-Res cells to the IKE-induced ferroptosis and its inhibition by ferrostatin-1. Results of cell viability assessment by the Live/Dead test (a, b) with representative images (c) in SH-SY5Y and SH-SY5Y-Res cells. "Ferro" is an activator of ferroptosis IKE (10 μM); "Ferro_Inh" is a combined use of the IKE activator (10 μM) and the ferroptosis inhibitor ferrostatin-1 (2 μM). Incubation period: 24 h (Ferrostatin-1 was added 1 hour before the addition of IKE). Data (a, b) are presented as mean ± standard deviation, $n = 4$; * $p < 0.05$, n.s. – not statistically significant (U-test).

and cellular respiration, than the parental cell population [19]. We therefore examined whether inhibition of these processes could facilitate overcoming resistance to RG7388. The hexokinase inhibitor 2-deoxyglucose was used to suppress glycolysis. Western blot and MTT analyses showed that 2-deoxyglucose alone induced cleavage of the apoptosis-associated proteins and markedly reduced viability of both parental and resistant cells. In combination with RG7388, 2-deoxyglucose increased cytotoxicity in both types of cells and led to overcoming resistance to MDM2 inhibition in SH-SY5Y-Res cells (Fig. 5, a and d). Similar effects were observed with rotenone, an inhibitor of ETC complex I (Fig. 5, b and e), and oligomycin, an ATP synthase inhibitor (Fig. 5, c and f). As single agents, both compounds induced apoptosis and reduced viability of parental and resistant cells. Both cell populations were more sensitive to rotenone than to oligomycin. Furthermore, the MDM2 inhibition-mediated cell death was increased in the presence of rotenone and oligomycin (Fig. 5, b, c, e, f).

Analysis of the efficacy of etoposide and other anticancer drugs for overcoming the resistance of malignant cells to MDM2 inhibition. We previously showed that SH-SY5Y-Res cells exhibit lower sensitivity to the chemotherapeutic drugs doxorubicin and cisplatin and that combining RG7388 with either cisplatin or selective antagonists of the antiapoptotic Bcl-2 family proteins allows partial overcoming of this type of resistance [19]. In the present study, we examined whether other anticancer agents could facilitate overcoming of resistance to RG7388. Similar to doxorubicin and cisplatin, etoposide is a DNA-damaging agent that inhibits topoisomerase II [41]. Etoposide was less effective in resistant SH-SY5Y-Res cells than in parental cells. It was shown using the MTT assay that the

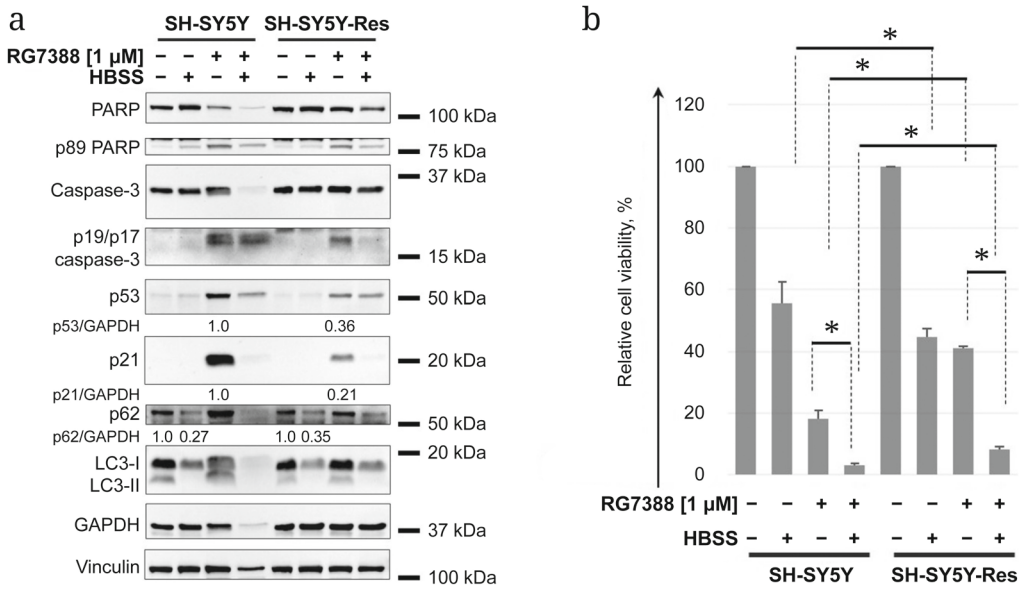

Fig. 4. Comparative analysis of the sensitivity of SH-SY5Y and SH-SY5Y-Res cells to autophagy activation by cultivation in HBSS in the presence and absence of RG7388. Results of Western blot analysis (a) and MTT assay (b) in SH-SY5Y and SH-SY5Y-Res cells. Incubation period: 24 h (HBSS medium was added 1 h before addition of the MDM2 antagonist). Data (b) are presented as a mean ± standard deviation, $n = 4$; * $p < 0.05$ (U-test).

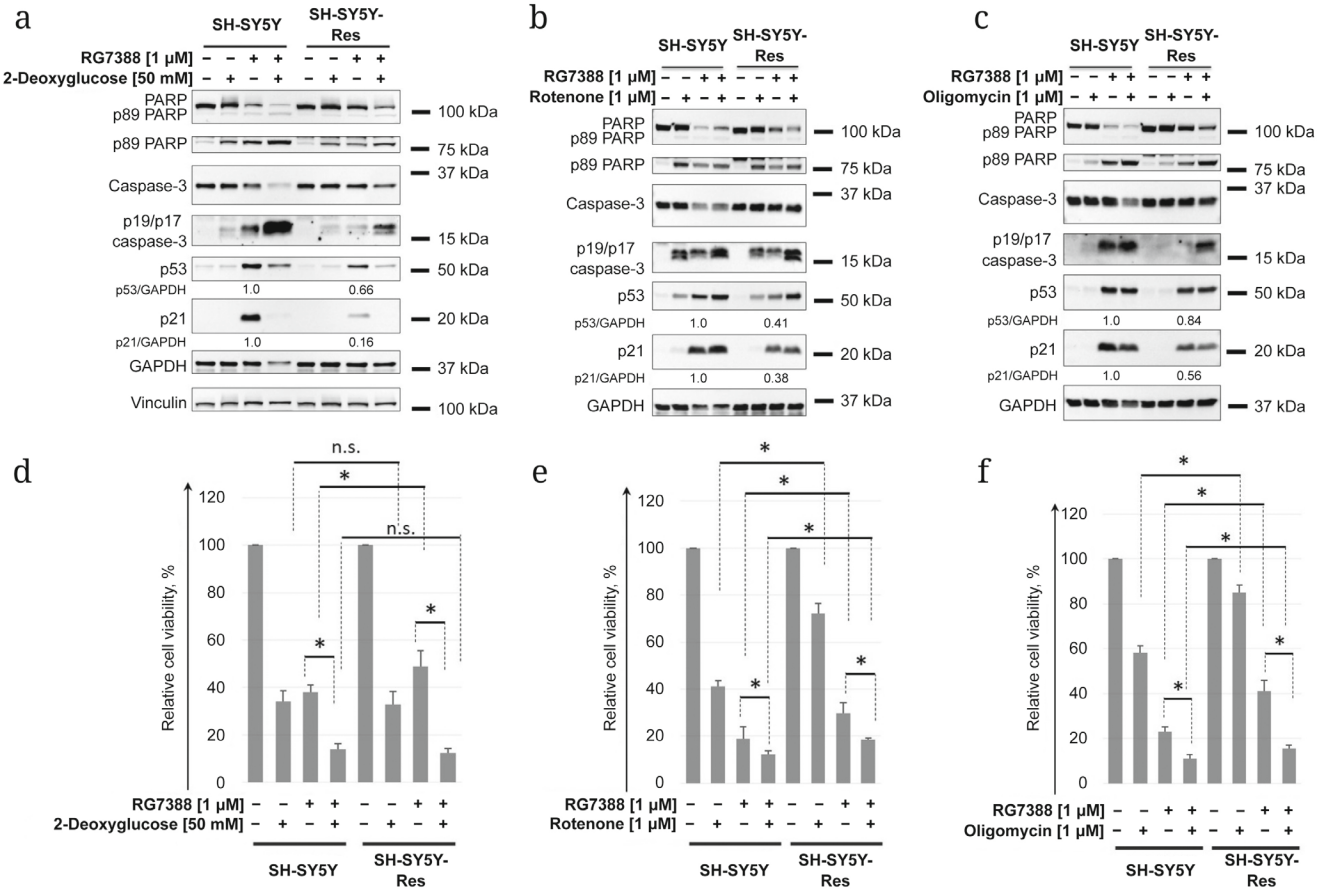

Fig. 5. Evaluation of the efficacy of 2-Deoxyglucose (a, d), Rotenone (b, e), and Oligomycin (c, f) in overcoming resistance of the SH-SY5Y neuroblastoma cells to RG7388. Results of Western blot analysis (a-c) and MTT test (d-f) of SH-SY5Y and SH-SY5Y-Res cells. Incubation period: 24 h. Data (d-f) are presented as the mean ± standard deviation, $n = 4$; * $p < 0.05$, n.s. – not statistically significant (U-test).

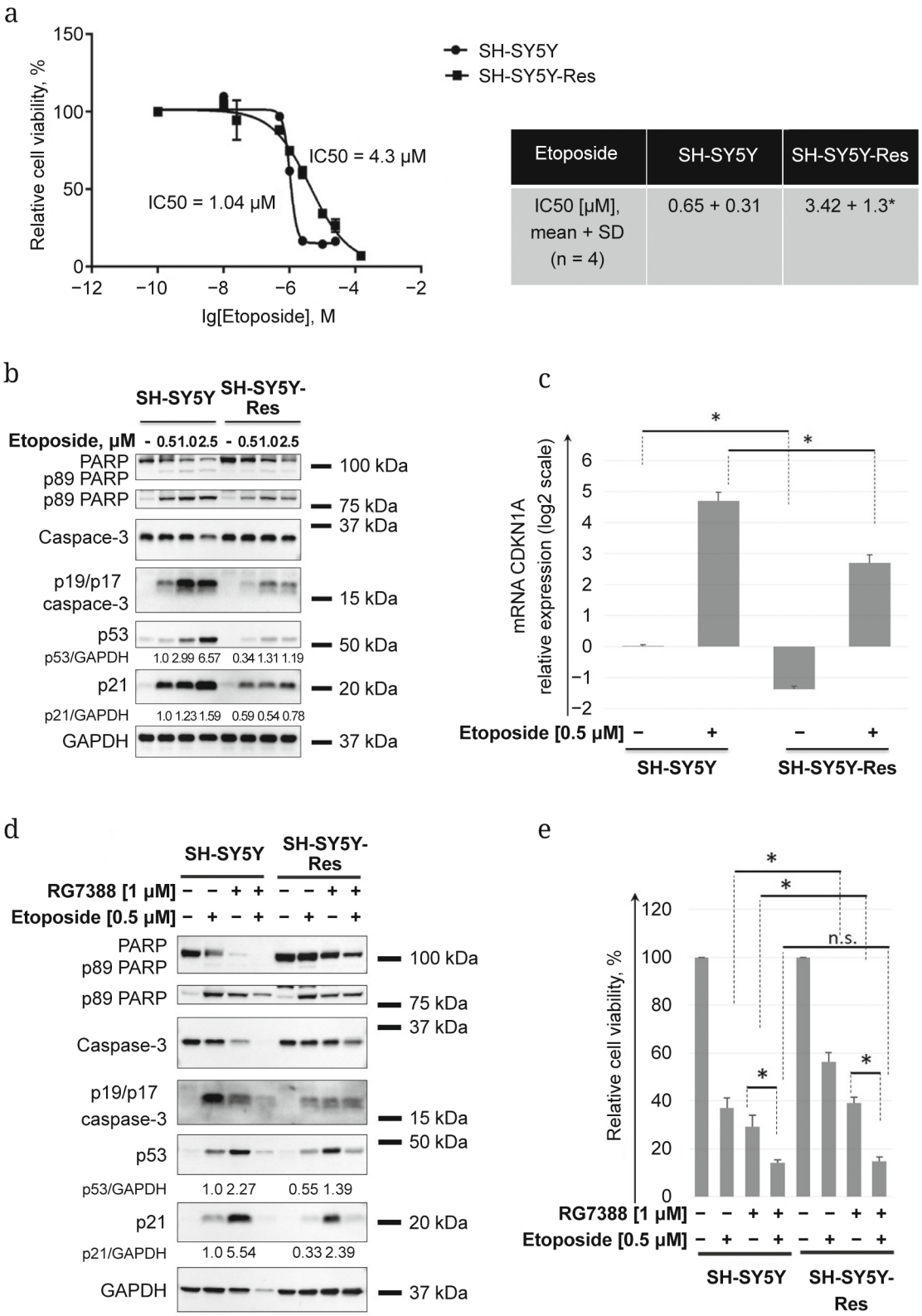

Etoposide	SH-SY5Y	SH-SY5Y-Res
IC50 [μM], mean + SD (n = 4)	0.65 + 0.31	3.42 + 1.3*

Fig. 6. Evaluation of the efficacy of Etoposide to overcome resistance of SH-SY5Y neuroblastoma cells to RG7388. Results of the MTT test (a, e), Western blotting analysis (b, d), and real-time PCR of the *CDKN1A* gene (p21 protein) (c) in SH-SY5Y and SH-SY5Y-Res cells. Incubation period: 24 h. log2 – logarithm to base 2. Data (a, c, e) are presented as a mean ± standard deviation, $n = 4$; * $p < 0.05$, n.s. – statistically not significant (U-test).

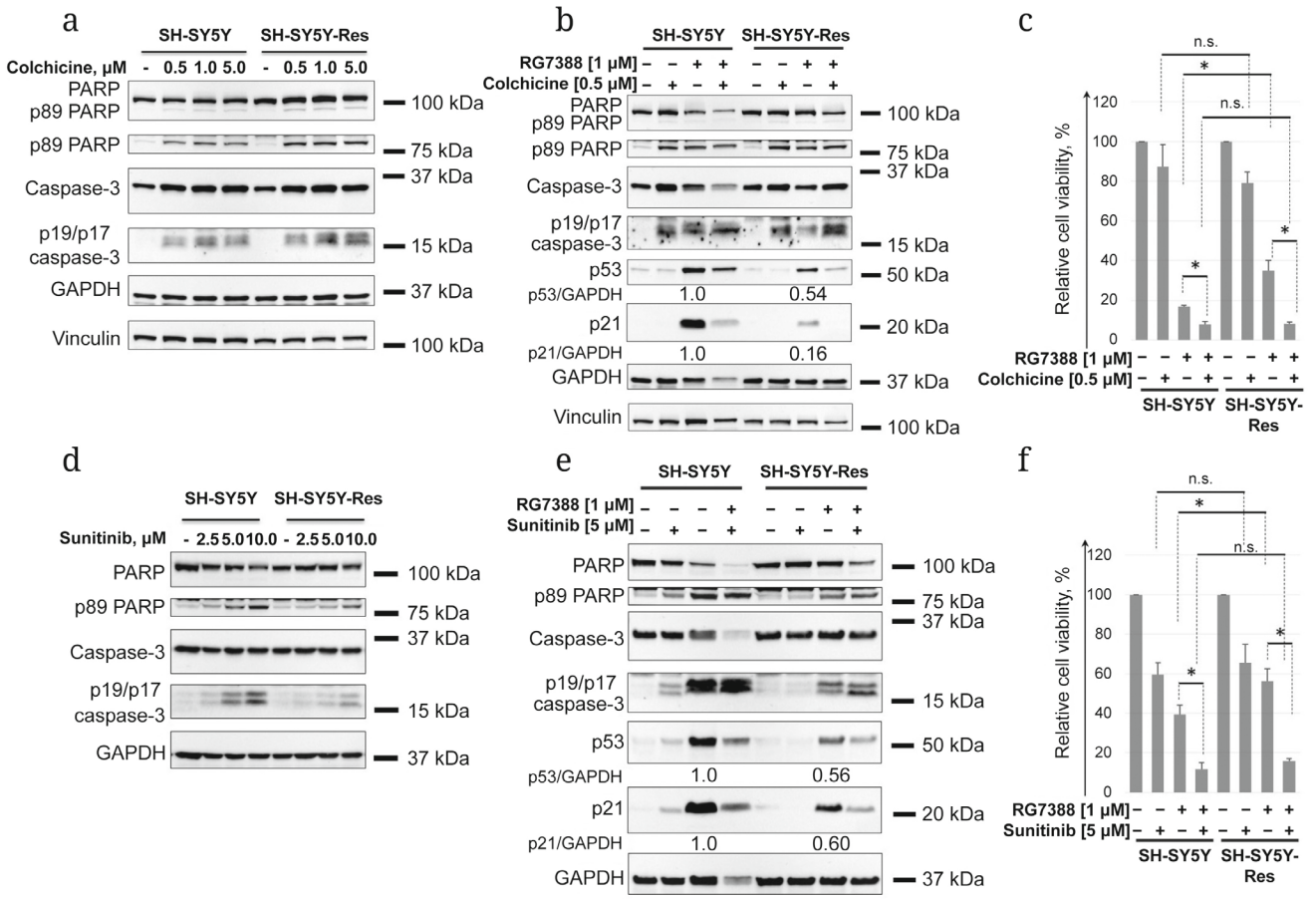

Fig. 7. Evaluation of the efficacy of colchicine (a-c) and sunitinib (d-f) in overcoming resistance of SH-SY5Y neuroblastoma cells to RG7388. Results of Western blot analysis (a, b, d, e) and MTT test (c, f) in SH-SY5Y and SH-SY5Y-Res cells. Incubation period: 24 h. Data (c, e) are presented as a mean ± standard deviation, $n = 4$; * $p < 0.05$, n.s. – not statistically significant (U-test).

IC_{50} of etoposide was approximately four-fold higher in resistant cells (Fig. 6a). Results of Western blotting confirmed this lower sensitivity based on the extent of caspase-3 processing and PARP cleavage. In addition, etoposide induced lower accumulation of p53 and p21 proteins in resistant cells, similar to the observed with RG7388 (Fig. 6b). The results of real-time PCR also revealed lower basal and etoposide-induced p21 mRNA levels (Fig. 6c), consistent with our previous findings for the MDM2 antagonist [19].

Western blotting and MTT analyses showed that combining etoposide with RG7388 increased the RG7388-induced cell death to a similar extent in parental and resistant cells. This combination eliminated in SH-SY5Y-Res cells resistance to RG7388 (Fig. 6, d and e).

Considering that the RG7388-resistant SH-SY5Y cells exhibited not only increased metabolism but also enhanced proliferative activity, the feasibility of using the antimitotic agent colchicine and the multikinase inhibitor sunitinib was assessed. The results of Western blot and MTT analyses showed no statistically significant differences between parental and resistant cells in their sensitivity to either compound when each was used as a single agent (Fig. 7).

However, when combined with RG7388, both colchicine and sunitinib effectively increased RG7388-induced death in both parental and resistant cells and suppressed their viability to a similar extent (Fig. 7).

DISCUSSION

Development of acquired drug resistance is a major challenge in advanced biomedicine. Malignant cells could acquire properties that allow them to evade toxic effects of anticancer compounds, thereby promoting cancer progression and reducing patient survival [42]. As noted above, targeting p53 to restore its tumor-suppressive activity represents a promising strategy for cancer therapy and has been actively studied throughout the twenty-first century [5]. The first MDM2 antagonists, members of the nutlin family, were introduced in 2004 [43].

The lead compound, Nutlin-3a, was subsequently modified to generate RG7112, the first MDM2 antagonist to enter clinical trials [44]. Despite its high anticancer activity in several preclinical models, RG7112 showed limited efficacy in clinical trials and caused adverse effects, probably because some normal cells are highly sensitive to the elevated p53 levels. RG7388, which was used in the present study and has been evaluated in clinical trials, has higher affinity for MDM2 than RG7112 [45]. Several other highly selective MDM2 antagonists, including APG-115 [46], AMG232 [47], and milademetan [48], have also entered clinical trials. However, many of these trials have been completed or discontinued for similar reasons. Limited efficacy and pronounced toxicity have so far prevented the MDM2 antagonists from being approved for clinical use [3, 4, 42].

Importantly, limited efficacy of these compounds could also be associated with the emergence of diverse mutations in the *TP53* gene. These include missense mutations, which result in single amino acid substitutions, and nonsense or other truncating mutations, which disrupt protein synthesis and produce shortened p53 variants. Other alterations include in-frame insertions or deletions and splice-site mutations that affect RNA maturation. Missense mutations are the most common alterations detected in the *TP53* gene. They could disrupt interaction between p53 and DNA, as occurs with the contact mutations, thereby impairing p53 activity, and/or induce conformational changes that reduce its structural stability [49]. In some cases, contact mutations increase p53 stability and promote its accumulation in the tumor cells [50].

We found that the His193Arg mutation in p53 is conformational. The mutant protein retains its ability to interact with DNA but does so less efficiently than the p53 protein in parental neuroblastoma cells [19]. The published data also indicate that this mutation reduces p53 stability [51-53]. Densitometric analysis of Western blots supported this finding. Both RG7388-induced p53 accumulation and basal p53 levels were lower in resistant cells than in parental counterparts (Fig. S5 in the Online Resource 1).

GAPDH and/or vinculin were used as loading controls in this study. It is known that GAPDH is a key glycolytic enzyme, and its expression could be altered by mutant p53 as part of the gain-of-function phenotype described above [54]. However, densitometric analysis showed no difference in GAPDH levels between SH-SY5Y-Res and parental neuroblastoma cells (Fig. S6 in the Online Resource 1). Vinculin was also assessed as an additional loading control in several experiments (Figs. 4a, 5a, and 7, a and b, and Fig. S4, a and b, in the Online Resource 1). Importantly, vinculin levels showed the same pattern as GAPDH.

We also demonstrated that the p53 mutation selected during continuous exposure to an MDM2 antagonist occurs spontaneously in tumors of different origins [19]. It is therefore important to investigate strategies for overcoming drug resistance in tumor cells carrying this mutation. In the present study, we further characterized the acquired resistance to MDM2 inhibition by RG7388. We previously showed that combining RG7388 with the antagonists of anti-apoptotic proteins could be effective. Here, we found that the basal levels of the major proapoptotic and antiapoptotic proteins did not differ significantly between the resistant and parental cell populations. We also analyzed cell-cycle alterations associated with acquisition of resistance. The increased proportion of SH-SY5Y-Res cells in the G1 phase indicates that acquisition of the resistant phenotype altered the basal cell-cycle distribution. However, this redistribution cannot be interpreted as classical p21-dependent arrest because it was accompanied by a decrease in the basal level of p21 mRNA, which mediates the p53-dependent G1 arrest [55]. Considering our previous findings concerning the His193Arg mutation in p53, impaired p53 transcriptional activity, and increased proliferative and metabolic activity in SH-SY5Y-Res cells [19], the increased G1 fraction possibly reflects changes in cell cycle control rather than reduced proliferative capacity.

The next step was the assessment of the possible contribution of other forms of PCD to the acquired resistance to MDM2 inhibitors. Neither cell type was sensitive to necroptosis induction, a caspase-independent form of PCD with necrotic morphological features [56, 57]. A key step in necroptosis is necrosome formation. The RIPK3–MLKL complex is an essential component of this process in all necroptotic pathways [58]. RIPK3 phosphorylates MLKL, thereby initiating pore formation and permeabilization of the plasma membrane [59]. Lack of sensitivity to TBZ-induced necroptosis is consistent with previous findings in SH-SY5Y neuroblastoma cells. Despite the reduced activity of caspase-8, which inhibits RIPK1 and RIPK3 [60], induction of cell death through the TNF-α pathway is not always possible in SH-SY5Y cells. This could be explained by the low basal levels of RIPK3 and MLKL [61, 62].

In contrast, SH-SY5Y cells responded to the induction of ferroptosis, another form of regulated necrotic cell death initiated by iron-dependent lipid peroxidation [63]. Interestingly, this response was attenuated in SH-SY5Y-Res cells, consistent with the evidence that chemoresistance could involve evasion not only of apoptosis but also of other forms of PCD, including ferroptosis [64], as previously shown for cisplatin resistance [37].

Autophagy, the process by which damaged intracellular organelles are degraded, and which could

underlie autophagic PCD, may also contribute to drug resistance by either promoting or limiting cellular response to chemotherapy [37, 65]. Parental and MDM2 inhibitor-resistant neuroblastoma cells differed in their sensitivity to autophagy induction during growth in HBSS. Moreover, these conditions markedly increased RG7388-induced cell death. Therefore, autophagy activation could represent a potential strategy for overcoming this type of resistance. However, the response to the autophagy inhibition differed between bafilomycin A1 and chloroquine and depended on their cytotoxicity. In parental SH-SY5Y cells, both inhibitors reduced cell viability to a similar extent and moderately increased the cytotoxicity of RG7388. Resistant cells were more sensitive to bafilomycin A1 than to chloroquine, and only bafilomycin A1 increased RG7388-induced cytotoxicity.

Metabolic alterations could also be associated with the acquired drug resistance, although the direction of these changes may vary. We previously found increased glycolytic and respiratory activity in the resistant clones compared with parental cells [19]. Therefore, several inhibitors of cellular metabolism were tested in the present study. The glycolysis inhibitor 2-deoxyglucose could either increase or decrease the tumor cells' sensitivity to chemotherapy, depending on tumor type [66]. Both SH-SY5Y and SH-SY5Y-Res cells were sensitive to 2-deoxyglucose, oligomycin, and rotenone as single agents. When combined with RG7388, these compounds enhanced RG7388-induced cytotoxicity and facilitated partial or complete overcoming of resistance. Consequently, inhibition of glycolysis or cellular respiration could represent a potential strategy for overcoming resistance to MDM2 inhibition.

In our previous study, the DNA-damaging drugs cisplatin and doxorubicin were shown to be less effective in the treatment of SH-SY5Y-Res cells both *in vitro* and *in vivo*. In the present study, we evaluated another agent from this group, etoposide, which is widely used to treat neuroblastoma [67]. Like the previously tested chemotherapeutic agents, etoposide was less cytotoxic as a single agent in SH-SY5Y-Res cells than in parental counterparts. However, in combination with RG7388, it showed similar efficacy in parental and resistant cells. Nevertheless, these findings illustrate another potential risk associated with this type of resistance. In addition to the adverse effects and limited efficacy described above, prolonged treatment with MDM2 antagonists could facilitate selection for more malignant clones with metabolic and proliferative adaptations. These clones could also be resistant to the conventional chemotherapeutic agents used to treat the same tumor type. Ultimately, this process could promote disease progression and relapses and contribute to poor patient survival.

Finally, because the resistant clones showed high proliferative activity, several compounds that inhibit cell division were tested. The antimitotic agent colchicine and the multikinase inhibitor sunitinib enhanced RG7388-induced cytotoxicity in both SH-SY5Y and SH-SY5Y-Res cells, thus overcoming resistance to RG7388. Therefore, antiproliferative agents might also be useful for overcoming this type of resistance.

CONCLUSION

SH-SY5Y neuroblastoma cell model was used to identify potential strategies for overcoming acquired resistance to the MDM2 antagonist RG7388. Resistant clones were less sensitive to the IKE-induced ferroptosis and showed an altered basal cell-cycle distribution, with a larger G1 fraction than parental SH-SY5Y cells. DNA-damaging agent etoposide was less effective as a single agent in SH-SY5Y-Res cells, but resistance to RG7388 was eliminated when used in combination with this compound. Autophagy activation increased RG7388-induced cytotoxicity in resistant cells, whereas the response of SH-SY5Y-Res cells to autophagy inhibition depended on whether chloroquine or bafilomycin A1 was used. The metabolic inhibitors 2-deoxyglucose, rotenone, and oligomycin also increased RG7388-induced cell death in SH-SY5Y-Res cells. Finally, combining the proliferation inhibitors colchicine or sunitinib with RG7388 could increase RG7388-induced cytotoxicity. Further studies are needed to determine how these combinations could be used to develop effective strategies for overcoming tumor cells' resistance to MDM2 inhibitors.

Abbreviations

Bcl-2	B-cell lymphoma 2
GAPDH	glyceraldehyde-3-phosphate dehydrogenase
HBSS	Hanks' balanced salt solution
IKE	imidazole ketone erastin
MDM2	mouse double minute 2 homolog
MDMX/MDM4	mouse double minute 4/X homolog
PARP	poly(ADP-ribose) polymerase
PCD	programmed cell death
PCR	polymerase chain reaction
TBZ	combination of TNF-α, BV6, and zVAD
TNF-α	tumor necrosis factor alpha

Supplementary information

The online version contains supplementary material available at https://doi.org/10.1134/S0006297926601875.

Acknowledgments

PCR experiments were performed at the facilities of Lomonosov Moscow State University.

Contributions

N.V.P., B.Z., and G.S.K. conceived and supervised the study. N.V.P. and E.S.P. performed the experiments. All authors discussed the results. N.V.P. and E.S.P. drafted the manuscript and prepared the figures. B.Z. and G.S.K. revised the manuscript.

Funding

This work was supported by a grant from the Russian Science Foundation (23-74-30006). Research was also supported (to B.Z.) by grants from the Swedish Cancer Society (222013) and the Stockholm Cancer Society (181301).

Conflict of interest

The authors declare that they do not have conflicts of interest.

Ethics approval and consent to participate

This article does not report any studies involving human participants or animals conducted by any of the authors.

REFERENCES

1. Hanahan, D. (2022) Hallmarks of cancer: new dimensions, *Cancer Discov.*, **12**, 31-46, https://doi.org/10.1158/2159-8290.CD-21-1059.
2. Mustafa, M., et al. (2024) Apoptosis: a comprehensive overview of signaling pathways, morphological changes, and physiological significance and therapeutic implications, *Cells*, **13**, 1838, https://doi.org/10.3390/cells13221838.
3. Fallatah, M. M. J., et al. (2023) Small-molecule correctors and stabilizers to target p53, *Trends Pharmacol. Sci.*, **44**, 274-289, https://doi.org/10.1016/j.tips.2023.02.007.
4. Hassin, O., et al. (2023) Drugging p53 in cancer: one protein, many targets, *Nat. Rev. Drug Discov.*, **22**, 127-144, https://doi.org/10.1038/s41573-022-00571-8.
5. Wang, W., et al. (2026) p53: from understanding its structure to advances in therapeutic targeting, *Signal Transduct. Targeted Ther.*, **11**, 121, https://doi.org/10.1038/s41392-025-02549-5.
6. Attardi, L. D., et al. (2026) p53: defender of lineage fidelity and foe of plasticity in cancer and regeneration, *Trends Cancer*, **12**, 542-552, https://doi.org/10.1016/j.trecan.2026.02.004.
7. Levine, A. J. (2020) p53: 800 million years of evolution and 40 years of discovery, *Nat. Rev. Cancer*, **20**, 471-480, https://doi.org/10.1038/s41568-020-0262-1.
8. Russano, F., et al. (2025) MDM2 in tumor biology and cancer therapy: a review of current clinical trials, *Int. J. Mol. Sci.*, **27**, 99, https://doi.org/10.3390/ijms27010099.
9. Wade, M., et al. (2012) Functional analysis and consequences of Mdm2 E3 ligase inhibition in human tumor cells, *Oncogene*, **31**, 4789-4797, https://doi.org/10.1038/onc.2011.625.
10. Carter, S., et al. (2007) C-terminal modifications regulate MDM2 dissociation and nuclear export of p53, *Nat. Cell Biol.*, **9**, 428-435, https://doi.org/10.1038/ncb1562.
11. Karni-Schmidt, O., et al. (2016) The roles of MDM2 and MDMX in cancer, *Annu. Rev. Pathol.*, **11**, 617-644, https://doi.org/10.1146/annurev-pathol-012414-040349.
12. Marine, J.-C., et al. (2016) MDMX (MDM4), a promising target for p53 reactivation therapy and beyond, *Cold Spring Harb. Perspect. Med.*, **6**, a026237, https://doi.org/10.1101/cshperspect.a026237.
13. Wu, H. H., et al. (2026) Targeting mutant p53 in cancer: from mechanistic insights to therapeutic strategies, *Cell. Mol. Biol. Lett.*, **31**, 87, https://doi.org/10.1186/s11658-026-00907-x.
14. Brown, A. L., et al. (2026) The Structure, pathogenesis, and inhibition of the p53-MDM2 pathway, *Cancers*, **18**, 546, https://doi.org/10.3390/cancers18040546.
15. Yu, D.-H., et al. (2020) Targeting MDMX for cancer therapy: rationale, strategies, and challenges, *Front. Oncol.*, **10**, 1389, https://doi.org/10.3389/fonc.2020.01389.
16. Haronikova, L., et al. (2021) Resistance mechanisms to inhibitors of p53-MDM2 interactions in cancer therapy: can we overcome them? *Cell. Mol. Biol. Lett.*, **26**, 53, https://doi.org/10.1186/s11658-021-00293-6.
17. Skalniak, L., et al. (2018) Prolonged Idasanutlin (RG7388) Treatment leads to the generation of p53-mutated cells, *Cancers*, **10**, 396, https://doi.org/10.3390/cancers10110396.
18. Berberich, A., et al. (2019) Targeting resistance against the MDM2 inhibitor RG7388 in glioblastoma cells by the MEK inhibitor trametinib, *Clin. Cancer Res.*, **25**, 253-265, https://doi.org/10.1158/1078-0432.CCR-18-1580.
19. Pervushin, N. V., et al. (2024) BH3-mimetics or DNA-damaging agents in combination with RG7388 overcome p53 mutation-induced resistance to MDM2 inhibition, *Apoptosis*, **29**, 2197-2213, https://doi.org/10.1007/s10495-024-02014-8.
20. Butera, A., et al. (2025) Deciphering the significance of p53 mutant proteins, *Trends Cell Biol.*, **35**, 258-268, https://doi.org/10.1016/j.tcb.2024.06.003.

21. Pitolli, C., et al. (2019) Do mutations turn p53 into an oncogene? *Int. J. Mol. Sci.*, **20**, 6241, https://doi.org/10.3390/ijms20246241.
22. Alvarado-Ortiz, E., et al. (2020) Mutant p53 gain-of-function: role in cancer development, progression, and therapeutic approaches, *Front. Cell Dev. Biol.*, **8**, 607670, https://doi.org/10.3389/fcell.2020.607670.
23. Gongalsky, M. B., et al. (2025) Amphiphilic photoluminescent porous silicon nanoparticles as effective agents for ultrasound-amplified cancer therapy, *ACS Appl. Mater. Interf.*, **17**, 374-385, https://doi.org/10.1021/acsami.4c15725.
24. Pervushin, N. V., et al. (2025) Mechanisms and ways to overcome acquired resistance of cancer cells to Mcl-1 antagonists, *Biochemistry (Moscow)*, **90**, 2009-2026, https://doi.org/10.1134/S0006297925602710.
25. Tweddle, D. A., et al. (2001) p53 cellular localization and function in neuroblastoma: evidence for defective G(1) arrest despite WAF1 induction in MYCN-amplified cells, *Am. J. Pathol.*, **158**, 2067-2077, https://doi.org/10.1016/S0002-9440(10)64678-0.
26. Van Goethem, A., et al. (2017) Dual targeting of MDM2 and BCL2 as a therapeutic strategy in neuroblastoma, *Oncotarget*, **8**, 57047-57057, https://doi.org/10.18632/oncotarget.18982.
27. Van Maerken, T., et al. (2014) Pharmacologic activation of wild-type p53 by nutlin therapy in childhood cancer, *Cancer Lett.*, **344**, 157-165, https://doi.org/10.1016/j.canlet.2013.11.002.
28. Sazonova, E. V., et al. (2024) Cancer drug resistance: targeting proliferation or programmed cell death, *Cells*, **13**, 388, https://doi.org/10.3390/cells13050388.
29. Senichkin, V. V., et al. (2021) Bak and Bcl-xL participate in regulating sensitivity of solid tumor derived cell lines to Mcl-1 inhibitors, *Cancers*, **14**, 181, https://doi.org/10.3390/cancers14010181.
30. McDermott, M., et al. (2014) *In vitro* development of chemotherapy and targeted therapy drug-resistant cancer cell lines: a practical guide with case studies, *Front. Oncol.*, **4**, 40, https://doi.org/10.3389/fonc.2014.00040.
31. Crowley, L. C., et al. (2016) Dead cert: measuring cell death, *Cold Spring Harb. Protocols*, **2016**, pdb.top070318, https://doi.org/10.1101/pdb.top070318.
32. Lazebnik, Y. A., et al. (1994) Cleavage of poly(ADP-ribose) polymerase by a proteinase with properties like ICE, *Nature*, **371**, 346-347, https://doi.org/10.1038/371346a0.
33. Fischer, M., et al. (2014) The transcription factor p53: not a repressor, solely an activator, *Cell Cycle*, **13**, 3037-3058, https://doi.org/10.4161/15384101.2014.949083.
34. Gottesman, M. M., et al. (1996) P-glycoprotein and multidrug resistance, *Curr. Opin. Genet. Dev.*, **6**, 610-617, https://doi.org/10.1016/s0959-437x(96)80091-8.
35. Maji, S., et al. (2018) Bcl-2 antiapoptotic family proteins and chemoresistance in cancer, *Adv. Cancer Res.*, **137**, 37-75, https://doi.org/10.1016/bs.acr.2017.11.001.
36. Pervushin, N. V., et al. (2023) Bcl-B: an "unknown" protein of the Bcl-2 family, *Biol. Direct*, **18**, 69, https://doi.org/10.1186/s13062-023-00431-4.
37. Pervushin, N. V., et al. (2024) Cisplatin resistance and metabolism: simplification of complexity, *Cancers*, **16**, 3082, https://doi.org/10.3390/cancers16173082.
38. Pervushin, N. V., et al. (2020) Nutrient deprivation promotes MCL-1 degradation in an autophagy-independent manner, *Biochemistry (Moscow)*, **85**, 1235-1244, https://doi.org/10.1134/S0006297920100119.
39. Yoshii, S. R., et al. (2017) Monitoring and measuring autophagy, *Int. J. Mol. Sci.*, **18**, 1865, https://doi.org/10.3390/ijms18091865.
40. Sazonova, E. V., et al. (2022) Drug toxicity assessment: cell proliferation versus cell death, *Cell Death Discov.*, **8**, 417, https://doi.org/10.1038/s41420-022-01207-x.
41. Baldwin, E., et al. (2005) Etoposide, topoisomerase II and cancer, *Curr. Med. Chem. Anti Cancer Agents*, **5**, 363-372, https://doi.org/10.2174/1568011054222364.
42. Wang, M., et al. (2026) Acquired resistance of cancer therapies: mechanisms and perspectives, *Chinese Med. J.*, **139**, 1272-1302, https://doi.org/10.1097/CM9.0000000000004048.
43. Vassilev, L. T., et al. (2004) *In vivo* activation of the p53 pathway by small-molecule antagonists of MDM2, *Science*, **303**, 844-848, https://doi.org/10.1126/science.1092472.
44. Vu, B., et al. (2013) Discovery of RG7112: a small-molecule MDM2 inhibitor in clinical development, *ACS Med. Chem. Lett.*, **4**, 466-469, https://doi.org/10.1021/ml4000657.
45. Ding, Q., et al. (2013) Discovery of RG7388, a potent and selective p53-MDM2 inhibitor in clinical development, *J. Med. Chem.*, **56**, 5979-5983, https://doi.org/10.1021/jm400487c.
46. Aguilar, A., et al. (2017) Discovery of 4-((3'R,4'S,5'R)-6″-chloro-4'-(3-chloro-2-fluorophenyl)-1'-ethyl-2″-oxodispiro[cyclohexane-1,2'-pyrrolidine-3',3″-indoline]-5'-carboxamido)bicyclo[2.2.2]octane-1-carboxylic acid (AA-115/APG-115): a potent and orally active murine double minute 2 (MDM2) inhibitor in clinical development, *J. Med. Chem.*, **60**, 2819-2839, https://doi.org/10.1021/acs.jmedchem.6b01665.

47. Erba, H. P., et al. (2019) Phase 1b study of the MDM2 inhibitor AMG 232 with or without trametinib in relapsed/refractory acute myeloid leukemia, *Blood Adv.*, **3**, 1939-1949, https://doi.org/10.1182/bloodadvances.2019030916.
48. Takahashi, S., et al. (2021) Safety and pharmacokinetics of milademetan, a MDM2 inhibitor, in Japanese patients with solid tumors: a phase I study, *Cancer Sci.*, **112**, 2361-2370, https://doi.org/10.1111/cas.14875.
49. Chen, X., et al. (2022) Mutant p53 in cancer: from molecular mechanism to therapeutic modulation, *Cell Death Dis.*, **13**, 974, https://doi.org/10.1038/s41419-022-05408-1.
50. Lozano, G., et al. (2025) Mutant p53 gain of function: why many see it, why some do not, *Cancer Discov.*, **15**, 1099-1104, https://doi.org/10.1158/2159-8290.CD-24-1638.
51. Monti, P., et al. (2011) Dominant-negative features of mutant TP53 in germline carriers have limited impact on cancer outcomes, *Mol. Cancer Res.*, **9**, 271-279, https://doi.org/10.1158/1541-7786.MCR-10-0496.
52. Di Como, C. J., et al. (1998) Human tumor-derived p53 proteins exhibit binding site selectivity and temperature sensitivity for transactivation in a yeast-based assay, *Oncogene*, **16**, 2527-2539, https://doi.org/10.1038/sj.onc.1202041.
53. Shi, Z., et al. (2011) Structural and functional impact of cancer-related missense somatic mutations, *J. Mol. Biol.*, **413**, 495-512, https://doi.org/10.1016/j.jmb.2011.06.046.
54. Butera, G., et al. (2018) Mutant p53 prevents GAPDH nuclear translocation in pancreatic cancer cells favoring glycolysis and 2-deoxyglucose sensitivity, *Biochim. Biophys. Acta Mol. Cell Res.*, **1865**, 1914-1923, https://doi.org/10.1016/j.bbamcr.2018.10.005.
55. Engeland, K. (2022) Cell cycle regulation: p53-p21-RB signaling, *Cell Death Differ.*, **29**, 946-960, https://doi.org/10.1038/s41418-022-00988-z.
56. Kopeina, G. S., et al. (2018) Programmed necrosis and tissue regeneration, *Genes Cells*, **13**, 35-38, https://doi.org/10.23868/201808017.
57. Yan, J., et al. (2022) Necroptosis and tumor progression, *Trends Cancer*, **8**, 21-27, https://doi.org/10.1016/j.trecan.2021.09.003.
58. Riebeling, T., et al. (2022) The role of RHIM in necroptosis, *Biochem. Soc. Transact.*, **50**, 1197-1205, https://doi.org/10.1042/BST20220535.
59. Xu, L., et al. (2025) Mixed lineage kinase domain-like protein (MLKL): from mechanisms to therapeutic opportunities, *Adv. Sci.*, **12**, e09277, https://doi.org/10.1002/advs.202509277.
60. Someda, M., et al. (2020) Caspase-8, receptor-interacting protein kinase 1 (RIPK1), and RIPK3 regulate retinoic acid-induced cell differentiation and necroptosis, *Cell Death Differ.*, **27**, 1539-1553, https://doi.org/10.1038/s41418-019-0434-2.
61. Vo, D.-K. H., et al. (2015) 24(S)-Hydroxycholesterol induces RIPK1-dependent but MLKL-independent cell death in the absence of caspase-8, *Steroids*, **99**, 230-237, https://doi.org/10.1016/j.steroids.2015.02.007.
62. Locquet, M.-A., et al. (2021) Caspase-8 deficiency induces a switch from TLR3 induced apoptosis to lysosomal cell death in neuroblastoma, *Sci. Rep.*, **11**, 10609, https://doi.org/10.1038/s41598-021-89793-1.
63. Dixon, S. J., et al. (2024) The cell biology of ferroptosis, *Nat. Rev. Mol. Cell Biol.*, **25**, 424-442, https://doi.org/10.1038/s41580-024-00703-5.
64. Zhang, C., et al. (2022) Ferroptosis in cancer therapy: a novel approach to reversing drug resistance, *Mol. Cancer*, **21**, 47, https://doi.org/10.1186/s12943-022-01530-y.
65. Niu, X., et al. (2025) Autophagy in cancer development, immune evasion, and drug resistance, *Drug Resist. Updates*, **78**, 101170, https://doi.org/10.1016/j.drup.2024.101170.
66. Maximchik, P., et al. (2018) 2-Deoxy-D-glucose has distinct and cell line-specific effects on the survival of different cancer cells upon antitumor drug treatment, *FEBS J.*, **285**, 4590-4601, https://doi.org/10.1111/febs.14687.
67. Imaya, M., et al. (2022) Combination chemotherapy consisting of irinotecan, etoposide, and carboplatin for refractory or relapsed neuroblastoma, *Cancer Med.*, **11**, 1956-1964, https://doi.org/10.1002/cam4.4529.

Publisher's Note. Pleiades Publishing remains neutral with regard to jurisdictional claims in published maps and institutional affiliations. AI tools may have been used in the translation or editing of this article.